Neural, Parallel, and Scientific Computations 16 (2008) 387-404

EXPONENTIAL TECHNIQUES AND IMPLICIT RUNGE-KUTTA METHODS FOR SINGULARLY-PERTURBED VOLTERRA INTEGRO-DIFFERENTIAL EQUATIONS

J. I. RAMOS

Room I-320-D, E. T. S. Ingenieros Industriales, Universidad de Málaga,
Plaza El Ejido, s/n, 29013 Málaga, SPAIN

ABSTRACT. Numerical experiments performed with an exponential finite difference method in equally-spaced and piecewise-uniform meshes for both the inner and the outer layers and with an implicit Runge-Kutta-Radau IIA method for the outer layer of singularly-perturbed Volterra integro-differential equations are reported. The exponential finite difference technique is based on piecewise linear approximations and its linear stability has been analyzed. It is shown that the exponential method presented in this paper provides first-order accurate solutions for small values of the perturbation parameter, whereas the same technique in a piecewise-uniform mesh is almost second-order uniformly convergent because it does resolve the inner layer and, most importantly, because the finite difference equations are independent of the perturbation parameter in the inner layer. The implicit Runge-Kutta method for the outer layer yields errors that only depend on the step size if the number of stages is small or the step size is large, but depend on both the small perturbation parameter and the step size, otherwise.

Key Words Singularly-perturbed Volterra integro-differential equations; exponentially finite difference methods; piecewise-uniform meshes; implicit Runge-Kutta methods.

1. PRELIMINARIES

Volterra's integro-differential equations arise in many fields such as, for example, mathematics, physics, engineering, etc. For example, initial-value problems of ordinary differential equations can be written as Volterra's integro-differential equations of the second kind and these equations are used to determine the existence and uniqueness of such equations by employing Picard's theorem [24]. Volterra's integro-differential equations also arise in models of population dynamics [10], epidemics [33], diffusion with nonlinear surface dissipation [26], synchronous control systems and nonlinear renewal processes [18], filament stretching [1], polymer rheology [25], nonlinear radiation heat transfer [23], etc.

Singularly-perturbed Volterra's integro-differential equations are characterized by the presence of a small, positive parameter that multiplies the first-order derivative of the dependent variable, and its singular character is due to the fact that the properties

Received January 30, 2008

of the solution for $\epsilon \neq 0$ are not compatible with those for $\epsilon = 0$, where ϵ denotes the small parameter. This incompatibility gives rise to the formation of an initial (or inner) layer where the solution adapts itself from the initial condition to the outer solution corresponding to $\epsilon = 0$, and has been the subject of several asymptotic analysis [2, 3, 27, 4, 5, 6].

Angell and Olmstead [2, 3] considered singularly-perturbed Volterra integral and integro-differential equations, respectively, with kernels which are sufficiently well-behaved or have an integrable singularity, respectively, by means of an asymptotic analysis of the inner and outer layers. For singularly-perturbed linear Volterra integral equations, Bijura [4] has shown that a discontinuity of the kernel causes layer solutions to decay algebraically rather than exponentially within the initial layer and that these solutions are similar to the Mittag-Leffler function.

Numerical methods for the solution of Volterra integro-differential equations include spectral techniques [12], spline collocation methods [20, 19, 7, 8], Petrov-Galerkin methods [28], implicit Runge-Kutta techniques [22], and exponential finite difference techniques [35, 29]. In particular, Salama and Bakr [35] developed an exponentially-fitted method [11] and determined the (fitting) coefficients of the finite difference discretization of the first-order derivative as suggested by Carroll [9], whereas those arising from the discretization of the integral term were determined from the analysis of the truncation errors. On the other hand, the author [29] employed a piecewise formulation based on the local linearization of the Volterra integro-differential equation which results in an exponential method and is exact for first-order linear ordinary differential with constant coefficients and linear right-hand sides [30]. He also considered a similar method but freezing the nonlinearities and solving the resulting nonlinear algebraic equations iteratively. Such an iterative (quasilinear) technique has been applied with great success for the analysis of singular initial– [31] and boundary-value [32] problems arising in classical and quantum mechanics.

In this paper, we first present a piecewise-quasilinearization method for Volterra integro-differential equations which result in exponential finite difference schemes, analyze its linear stability and show that some inconsistencies may arise between the leading-order outer analytical solution and the finite difference discretization as the small perturbation parameter tends to zero. We also show how to get consistency, even though, for the examples considered in the paper, no inconsistency arises. The exponential method is then combined with a Shishkin piecewise-uniform mesh [14, 34] and shown to result in a finite difference method that is independent of the small perturbation parameter in the inner layer. Finally, an implicit Runge-Kutta method is developed and applied to determine the solution in the outer layer using as initial conditions either those corresponding to the exact solution (when available) or those of the exponential method in piecewise-uniform meshes presented in this paper.

The paper has been organized as follows. In Section 2, the problem is formulated in its standard integro-differential form as well as a system of first-order ordinary differential equations, while, in Section 3, we present a piecewise quasilinear method and analyze its linear stability. Such a method is an extension of the quasilinear techniques developed by the author [29] where a detailed analysis of the discretization of the advection operator and the numerical treatment of integrals appearing in Volterra integro-differential equations and comparisons with the exponentially-fitted techniques of Salama and Bakr [35] are reported. In the same section, an exponential technique in piecewise-uniform meshes and an implicit Runge-Kutta technique are presented, whereas, in Section 4, the three techniques presented in the paper are applied to two examples which have analytical solutions and the results are compared with those obtained by means of the backward Euler and trapezoidal methods as well as with the most accurate technique reported by Salama and Bakr [35]. Finally, a brief summary of the main findings of the paper conclude the manuscript.

2. EXISTENCE OF EXTREMAL SOLUTIONS

Consider the following singularly-perturbed Volterra integro-differential equation

$$\epsilon y'(t) + a(t)y(t) = f(t, y(t)) + \int_0^t K(t, s, y(s))ds, \qquad t > 0, \tag{2.1}$$

where the prime denotes differentiation with respect to t, $0 < \epsilon \ll 1$, $a(t) > 0$ and $y(0) = y_0$, which can be written in autonomous form as

$$\epsilon y'(t) + a(t)y(t) = g\left(y(t), u(t,t)\right), \tag{2.2}$$

upon introducing $t' = 1$ and replacing $(t, y(t))$ by $y(t)$, where

$$u(t, \tau) = \int_0^t K(\tau, y(s))ds, \tag{2.3}$$

and, therefore, $u(0, \tau) = 0$.

We assume that a, f, K and, therefore, g are sufficiently smooth functions of its arguments, and that y_0, f and K may depend smoothly on ϵ although such a dependence is omitted here. Therefore, the existence and uniqueness of the solution of Eq. (2.1) follows from fixed-point theory.

Equation (2.1) can be written as a system of first-order ordinary differential equations in an infinite-dimensional Banach space upon differentiation of Eq. (2.3) with respect to t as

$$\begin{aligned} \epsilon y'(t) + a(t)y(t) &= g\left(y(t), u(t,t)\right), & y(0) &= y_0, \\ \frac{\partial u}{\partial t} &= K(\tau, y(t)), & u(0, \tau) &= 0, \end{aligned} \tag{2.4}$$

to which one can apply the results obtained by Hairer et al. [15, 16, 17] and thus obtain the corresponding results for Eq. (2.1). In particular, under the conditions stated above and for $0 \leq t \leq T$, Eq. (2.1) has a unique solution for sufficiently small ϵ which can be written as

$$y(t) = \sum_{n=0}^{N} \epsilon^n y_n(t) + \sum_{n=0}^{N} \epsilon^n Y_n\left(\frac{t}{\epsilon}\right) + O(\epsilon^{N+1}), \tag{2.5}$$

where the first and second terms correspond to the outer and inner expansions, respectively. For example,

$$y_0(t) = \frac{1}{a(t)}\left(f(t, y_0(t)) + \int_0^t K(t, s, y_0(s))ds\right),$$

$$y_1(t) = \frac{1}{a(t)}\left(-y_0'(t) + g_y(t, y_0(t))y_1(t) + g_u(t, y_0(t)) \int_0^t K_y(t, s, y_0(s))y_1(s)ds\right), \tag{2.6}$$

where the subscripts denote partial differentiation, the functions $Y_n\left(\frac{t}{\epsilon}\right)$ decay exponentially in the variable $\left(\frac{t}{\epsilon}\right)$, and the initial-layer thickness is $O(\epsilon)$. Note that Eq. (2.4) is a stiff system of ordinary differential equations.

3. NUMERICAL METHODS

As indicated in the Introduction, three different methods have been followed for solving Eq. (2.1). The first method is of exponential type, the second one uses the first method in a piecewise-uniform mesh, and the third one employs an implicit Runge-Kutta method for the outer layer; these methods are described in the following subsections.

Although not reported here, the second method was also applied to determine the solution in the inner layer whereas the solution in the outer layer was calculated from Eq. (2.1) with $\epsilon = 0$, i.e., with the leading-order term of the outer solution, and the differences between the results thus obtained and those corresponding to the second method were found to be very small for $\epsilon \leq 2^{-6}$ for the two examples described in Section 3, provided that the transition point between the inner and outer layers is sufficiently far away so that the initial layer behavior is over.

3.1. **Exponential methods.**

Equation (2.1) can be written as

$$\epsilon y'(t) + a(t)y(t) = G(t), \tag{3.1}$$

where

$$G(t) \equiv f(t, y(t)) + \int_0^t K(t, s, y(s))ds. \tag{3.2}$$

In the interval $[t_n, t_{n+1}]$, Eq. (3.1) can be integrated analytically to yield

$$y(t) = y_n \exp\left(-\int_{t_n}^{t} \frac{a(s)}{\epsilon} ds\right) + \frac{1}{\epsilon}\int_{t_n}^{t} \exp\left(-\int_{s}^{t} \frac{a(\tau)}{\epsilon} d\tau\right) G(s) ds. \tag{3.3}$$

If, in that interval, $a(t)$ is approximated by its Taylor series expansion, i.e., $a(t) = a(t^*)+b(t^*)(t-t^*)+O((t-t^*)^2)$, where t^* is the expansion point, it is an easy exercise to show that the selection $t^* = \frac{1}{2}(t_n + t_{n+1})$ eliminates the contribution of the $b = a'$ term to the integral $\int_{t_n}^{t_{n+1}} \frac{a(s)}{\epsilon} ds$. We, therefore, hereon assume that t^* has been selected as explained above, neglect the linear term in the Taylor series expansion of $a(t)$ about t^* and approximate $G(t)$ in $[t_n, t_{n+1}]$ with second-order accuracy by

$$G(t) = G_n + \frac{1}{h_n}(G_{n+1} - G_n)(t - t_n), \tag{3.4}$$

where $h_n = t_{n+1} - t_n$ is the local step size and $G_n = G(t_n)$.

Upon using these approximations, it is an easy matter to show that Eq. (3.3) yields

$$y_{n+1} = y_n \exp\left(-\frac{a_n^* h_n}{\epsilon}\right) + \frac{1}{a_n^*}\left(1 - \exp\left(-\frac{a_n^* h_n}{\epsilon}\right)\right)\left(G_n + \phi_n(G_{n+1} - G_n)\right), \tag{3.5}$$

where

$$\phi_n = \frac{1}{1 - \exp\left(-\frac{a_n^* h_n}{\epsilon}\right)} - \frac{\epsilon}{a_n^* h_n}, \tag{3.6}$$

$a_n^* = a\left(\frac{1}{2}(t_n + t_{n+1})\right)$, and G_n can be determined from a second-order accurate trapezoidal rule as, cf. Eq. (3.2),

$$G_n = f(t_n, y_n) + \frac{1}{2}\sum_{i=0}^{n-1}(K(t_n, t_i, y_i) + K(t_n, t_{i+1}, y_{i+1})h_i, \tag{3.7}$$

where $t_0 = 0$.

Substitution of Eq. (3.7) into Eq. (3.5) results in an algebraic equation for y_{n+1} which is nonlinear if either f or K are nonlinear functions of $y(t)$. Such nonlinear systems may be solved iteratively by means of the Newton-Raphson method.

It must be note that, as $\frac{a_n^* h_n}{\epsilon} \to \infty$, Eq. (3.5) implies that $y_{n+1} \to \frac{G_{n+1}}{a_n^*}$, whereas, in the limit $\epsilon \to 0$, Eq. (3.1) implies that $y(t) \to \frac{G(t)}{a(t)}$ which does not coincide with the expression obtained above at t_{n+1} unless $a_n^* = a_{n+1}$. If this value is considered, then Eq. (3.5) is still valid, but $\int_{t_n}^{t_{n+1}} a(s)ds = a_{n+1}h_n + O(h_n^2)$, whereas $\int_{t_n}^{t_{n+1}} a(s)ds = a(t_n^*)h_n + O(h_n^3)$ for $t_n^* = \frac{1}{2}(t_n + t_{n+1})$.

Remark 1. Consistency between the exponential method presented above and the leading-order analytical outer solution can be achieved by replacing $G_n + \phi_n(G_{n+1} - G_n)$ in Eq. (3.5) by $\beta G_n + \gamma G_{n+1}$ where $\beta = \frac{a_n^*}{a_n}(1 - \phi_n)$ and $\gamma = \frac{a_n^*}{a_{n+1}}\phi_n$, since $\lim_{\frac{a_n^* h_n}{\epsilon} \to \infty} \phi_n = 1$, and this amounts to replacing G_n and G_{n+1} in Eq. (3.5) by $\frac{a_n^*}{a_n}G_n$ and $\frac{a_n^*}{a_{n+1}}G_{n+1}$. Such an approximation has been followed by Il'in [21], Farrell [13]

and Carroll [9] for singularly-perturbed first-order ordinary differential equations and result in exponentially-fitted methods which are second-order uniformly convergent.

Remark 2. If $G(t)$ is approximated with first-order accuracy by G_n in $[t_n, t_{n+1}]$, Eq. (3.5) is valid provided that ϕ_n in that equation is set to zero. On the other hand, if $G(t)$ is approximated by G_{n+1} in $[t_n, t_{n+1}]$, Eq. (3.5) is valid provided that ϕ_n in that equation is set to unity. In either case, there is no consistency between the leading-order analytical outer solution and that of the exponential method considered above. Such a consistency can be achieved by approximating $G(t)$ by G_{n+1} and evaluating $a(t)$ at t_{n+1}; however, such an evaluation has a larger error than the evaluation of $a(t)$ at $t_n^* = \frac{1}{2}(t_n + t_{n+1})$, as discussed in Remark 1. Furthermore, the evaluation of $G(t)$ at either t_n or t_{n+1} corresponds to simple right-end and left-end rectangular quadrature rules for the integral in Eq. (2.1) both of which are less accurate than the trapezoidal rule considered in Eq. (3.7).

Remark 3. If the following approximations $a_n^* = a_n$ and $G(t) \approx G_n$ are made in Eq. (3.3), then the resulting method coincides with those proposed by Doolan et al. [11] and Eq. (24) of Farrell [13] for first-order ordinary differential equations. On the other hand, if $a_n^* = a_{n+1}$ and $G(t) \approx G_{n+1}$, one obtains the method proposed by Doolan et al. [11] and Eq. (29) of Farrell [13] for first-order ordinary differential equations. In both cases, the resulting finite difference methods do not satisfy the optimality condition $|y_n^h - y(t_n)| \leq C \min(\max_{0\leq j\leq n}(h_j^p, \epsilon))$, although they are uniformly convergent of order $O(h^2)$ [13] for singularly-perturbed first-order ordinary differential equations.

The first numerical method considered in this study for the solution of Eq. (2.1) employs Eqs. (3.5) and (3.7) in $0 \leq t \leq T$ where T denotes the (total) integration interval, i.e., Eqs. (3.5) and (3.7) are used in both the inner and the outer layers, and is here referred to as EIEO which may employ fixed or variable step sizes.

3.2. **Linear stability of EIEO.** The linear stability of the EIEO formulation presented above can be readily analyzed in equally-spaced grids by considering the following linear, homogeneous Volterra integro-differential equation

$$\epsilon y' + \lambda_1 y + \lambda_2 \int_0^t y(s)ds = 0, \qquad t > 0, \tag{3.8}$$

where λ_1 and λ_2 are constants and, according to the definitions introduced above, $a_n^* = \lambda_1$, $G = -\lambda_2 \int_0^t y(s)ds$, and (cf. Eq. (3.5))

$$\exp(\rho\lambda_1)y_{n+1} - y_n = \frac{1}{\lambda_1}(\exp(\rho\lambda_1) - 1)(G_n + \phi(G_{n+1} - G_n)), \tag{3.9}$$

where ϕ is now a constant (cf. Eq. (3.6)) and $\rho = \frac{h}{\epsilon}$, so that

$$\lambda_1 y_{n+1} - \lambda_1 \exp(-\rho\lambda_1) y_n = -\frac{1}{2}\lambda_2 h(1 - \exp(-\rho\lambda_1)) \sum_{j=1}^{n} (y_n + y_{n+1}), \tag{3.10}$$

and

$$\lambda_1 y_n - \lambda_1 \exp(-\rho\lambda_1) y_{n-1} = -\frac{1}{2}\lambda_2 h(1 - \exp(-\rho\lambda_1)) \sum_{j=1}^{n-1} (y_n + y_{n+1}). \tag{3.11}$$

Subtraction of Eqs. (3.10) and (3.11) yields

$$(\lambda_1 + \frac{1}{2}\lambda_2 h(1-\exp(-\rho\lambda_1)) y_{n+1} - \lambda_1(1+\exp(-\rho\lambda_1)) y_n + \lambda_1 \exp(-\rho\lambda_1) y_{n-1} = 0, \tag{3.12}$$

which is a linear difference equation with constant coefficients. Its solutions are of the form $u_i = C\mu^i$ where C is a constant and μ obeys a quadratic equation whose roots are

$$\mu_{1,2} = \frac{1}{2(\lambda_1 + \frac{1}{2}\lambda_2 h(1 - \exp(-\rho\lambda_1)))} (\lambda_1(1 + \exp(-\rho\lambda_1)) \pm \sqrt{R}), \tag{3.13}$$

where

$$\begin{aligned} R &= \lambda_1^2(1 + \exp(-\rho\lambda_1))^2 - 4\lambda_1 \exp(-\rho\lambda_1)(\lambda_1 + \frac{1}{2}\lambda_2 h(1 - \exp(-\rho\lambda_1))) \\ &= \lambda_1(1 - \exp(-\rho\lambda_1))(\lambda_1(1 - \exp(-\rho\lambda_1)) - 2\lambda_2 h \exp(-\rho\lambda_1)). \end{aligned} \tag{3.14}$$

If $R > 0$ and $\lambda_1 > 0$, it is an easy exercise to show that

$$0 < \mu_1 = \frac{\lambda_1}{\lambda_1 + \frac{1}{2}\lambda_2 h(1 - \exp(-\rho\lambda_1))} < 1, \tag{3.15}$$

and $0 < \mu_2 < 1$ provided that $\lambda_2 > 0$.

If $R < 0$ so that $\mu_{1,2}$ are complex conjugate, it is easy to show that

$$|\mu_{1,2}|^2 = \frac{\lambda_1 \exp(-\rho\lambda_1)}{\lambda_1 + \lambda_2 h(1 - \exp(-\rho\lambda_1))} < 1, \tag{3.16}$$

provided that λ_1 and λ_2 are positive.

$R = 0$ implies that $\lambda_2 h = \frac{\lambda_1}{2}(\exp(\rho\lambda_1) - 1)$ which, in turn, implies that $\mu_1 = \mu_2 = \frac{2}{\cosh(\rho\lambda_1)} < 1$. Therefore, the EIEO formulation presented in this paper is linearly stable.

Remark 4. It is readily shown that when the integral in Eq. (3.2) is approximated by a right-end rectangular quadrature rule, a linear stability analysis analogous to the one reported above shows that the resulting method is linearly stable and the roots of its characteristic polynomial can be simply obtained by replacing $\lambda_2/2$ by λ_2 in Eq. (3.12).

3.3. **Exponential methods in piecewise-uniform meshes.** As stated above, when Eq. (3.1) is a linear ordinary differential equation with $a(t)$ constant and $G(t)$ a linear function of t, then Eq. (3.5) provides the exact solution of that equation. However, for equally-spaced grids in both the inner and the outer layers and $\epsilon < h$, where h denotes the constant step size, Eq. (3.5) does not resolve the inner layer and its accuracy drops from second to first order for time-dependent $a(t)$ and $G(t)$.

In this section, we present an implementation of the exponential finite difference method presented above in a piecewise-uniform mesh. Such a mesh employs N_I and N_O equally-spaced intervals in the inner and outer layers, respectively, which result in grid spacings equal to h_I and h_O, respectively, as follows. A simple dominant balance argument in Eq. (3.1) indicates that the inner layer thickness $T_I = O(\frac{\epsilon}{\bar{a}})$ where $\bar{a} = \min(a(t))$ in $[0, T]$, where T is the total integration time which is assumed to be larger than T_I and, therefore, lies in the outer layer.

The total integration interval $[0, T]$ is divided into two non-overlapping intervals as $[0, T] = [0, T_I] \bigcup [T_I, T]$, where T_I can be set to $\alpha \frac{\epsilon}{\bar{a}}$ where $\alpha > 1$; therefore, $h_I = \frac{T_I}{N_I} = \frac{\alpha \epsilon}{N_I \bar{a}}$, $\lim_{N_I \to \infty} h_I = 0$, and the exponents that appear in Eq. (3.3) are independent of ϵ, i.e., Eq. (3.3) is independent of ϵ for the inner layer. The coordinates of the grid points in the inner and outer layers are $0 + nh_I$, $n = 0, 1, \ldots, N_I$, and $T_I + mh_O$, $m = 0, 1, \ldots, N_O$, respectively, and the grid spacing changes abruptly at $t = T_I$ from h_I to h_O for small ϵ, where $h_O = \frac{T - T_I}{N_O}$. Furthermore, the coordinates of the points in the outer layer can be expressed as $x_m = \frac{N_O - m}{N_O} T_I + \frac{m}{N_O} T$ for $m = 0, 1, \ldots, N_O$ where the two summands are non-negative.

For constant $a(t)$ and $G(t)$, i.e., $\bar{a} = a(t)$, the solution of Eq. (3.1) is $u(t) = \frac{G}{a} + \left(U - \frac{G}{a}\right) \exp\left(-\frac{at}{\epsilon}\right)$, where $U = u(0)$, and, therefore, in the inner layer, $\frac{a_I t_n}{\epsilon} = \frac{\alpha a_n n}{N_I \bar{a}} > 0$ which is independent of ϵ, whereas, in the outer layer $\frac{a_O t_n}{\epsilon} = \frac{\alpha a_n (N_O - m)}{N_I N_O \bar{a}} + \frac{\alpha a_n m T}{N_O} > 0$ and the ratio of the two summands is a monotonically increasing function of m which is equal to zero for $m = 0$ and ∞ for $m = N_O$. Furthermore, the first summand does not depend on ϵ, whereas the second one is very large except for $m = 0$ on account that ϵ is small and appears in the denominator and $T >> \frac{\epsilon}{\bar{a}}$; in fact, the dependence of the second summand on ϵ is exponentially small.

The exponential method in piecewise-uniform meshes described in the previous paragraphs depends on three parameters α, N_I and N_O. The selection of α must be made so that the inner layer lies in $[0, T_I]$ and $\alpha > 1$, whereas that of N_I should be made so that the inner layer is resolved and $\lim_{N_I \to \infty} h_I = O$ and that of N_O is based on accuracy considerations. Furthermore, α could be a function $\psi(N_I)$, e.g., $\alpha = \beta \psi(N_I)$, provided that $\lim_{N_I \to \infty} \frac{\psi(N_I)}{N_I} = O$ so that $\lim_{N_I \to \infty} h_I = O$.

Remark 5. It is interesting to point out that the piecewise-uniform mesh is related to Shishkin's piecewise-uniform grids for the numerical solution of two-point

boundary-value advection-diffusion equations [14] which are usually employed with upwind difference operators for the discretization of the advection terms [14]. In a Shishkin mesh, the interval $[0,T]$ is first mapped into $[0,1]$, and the latter is then divided into two equally-spaced subintervals $[0,\sigma]\bigcup[\sigma,1]$, and, in each subinterval, an equal number of grid points, $\frac{N}{2}$, is used, where $\sigma = \min\left(\frac{1}{2}, \frac{1}{\alpha}\epsilon \ln N\right)$, $a(t) \geq \alpha > 0$, $N+1$ is the number of grid points, and the grid spacing in the inner and outer layers are $h_I = \frac{2\sigma}{N}$ and $h_0 = \frac{2(1-\sigma)}{N}$, respectively. Note that, if $\frac{1}{2} < \frac{1}{\alpha}\epsilon \ln N$, then $h_I = h_0 = \frac{1}{N}$ and the mesh is equally-spaced throughout the whole integration interval. On the other hand, if $\frac{1}{2} > \frac{1}{\alpha}\epsilon \ln N$, $h_I = \frac{2\epsilon}{\alpha N}\ln N$ and $\frac{a_I^* h_I}{\epsilon} = \frac{2a_I^*}{\alpha N}\ln N$ which indicates that the local mesh Reynolds number is independent of ϵ for $[0,\sigma]$ and, therefore, Eq. (3.5) is independent of ϵ for the interior points of the inner layer. Moreover, if $\frac{1}{2} > \frac{1}{\alpha}\epsilon \ln N$, $\frac{1}{N} < h_O = \frac{2}{\alpha N}(1 - \frac{1}{\alpha}\epsilon \ln N) < \frac{2}{N}$ and $\frac{a_O^* h_O}{\epsilon} < \frac{a_0^*}{N\epsilon}$ and, therefore, the term $\exp\left(-\frac{a_O^* h_O}{\epsilon}\right)$ in Eq. (3.5) tends to zero as $\epsilon \to 0$, i.e., the outer solution is obtained (cf. Eq. (3.5) and Remark 1). Hereon, we shall refer to the exponential method in piecewise-uniform meshes described above as EPUM. Note that the mesh spacing changes abruptly at $n = \frac{N}{2}$ from h_I to h_0 for small values of ϵ.

Remark 6. The precise choice of the mesh transition point, σ, in a Shishkin piecewise uniform mesh is of paramount importance both theoretically and numerically. For example, when such a mesh is used with upwind for the convection terms for one-dimensional linear convection-diffusion equations, uniform convergence requires that σ should behave as $\frac{k}{\alpha}\epsilon\phi(N)$ where $\phi(N) \to \infty$, but $\frac{1}{N}\phi(N) \to 0$ as $N \to \infty$ and k is a positive constant. The simplest choice for $\phi(N)$ that satisfies the above requirements is $\ln(N)$. Some authors have employed $k = 2$ and the choice of the optimal value of k has been discussed by Stynes and Tobiska [36], for one-dimensional convection-diffusion equations. For these equations, it must be noted that a Shishkin piecewise-uniform mesh may not fully resolve the boundary layer because the absolute value of the first-order derivative may be large in $[x_{\frac{N}{2}-1}, x_{\frac{N}{2}}]$.

Remark 7. The piecewise-uniform meshes described above do require a knowledge of the order of the initial layer thickness (a similar comment applies to convection-dominated flows) and, in the long run, may be superseded by adaptive numerical methods whereby a solution on some conventional mesh is first obtained by means of a stable numerical technique and then used to compute local error estimators which provide some guidance on where the original mesh should be refined or coarsened so that the new mesh is better fitted for the problem. On this new mesh, one may then obtain another solution to the problem, which is again modified based on the local error estimator, and this iterative process is continued until an appropriate stopping criterion is satisfied.

3.4. **Implicit Runge-Kutta method.** The implicit Runge-Kutta method considered in this study is based on the solution of the ordinary differential Eq. (2.4), rather than in Eq. (3.1). Consider an s-stage implicit Runge-Kutta method characterized by an invertible matrix whose elements are a_{ij} and the coefficients $(b_1, \ldots, b_s)$ and $(c_1, \ldots, c_s)$. If the approximations to $y(t_n)$ and $u(t_n, \tau)$ are denoted by y_n and $u_n(\tau)$, respectively, then

$$y_{n+1} = y_n + h_n \sum_{i=1}^{s} b_i Y'_{ni},$$

$$u_{n+1}(\tau) = u_n(\tau) + h_n \sum_{i=1}^{s} b_i U'_{ni}(\tau), \tag{3.17}$$

where

$$\epsilon Y'_{ni} = g(Y_{ni}, U_{ni}),$$

$$U'_{ni}(\tau) = K(\tau, Y_{ni}), \tag{3.18}$$

$t_{ni} = t_n + c_i h_n$.

The internal stages of the implicit Runge-Kutta method can be written as

$$Y_{ni} = y_n + h_n \sum_{j=1}^{s} a_{ij} Y'_{nj},$$

$$U_{ni}(\tau) = u_n + h_n \sum_{j=1}^{s} a_{ij} U'_{nj}(\tau), \tag{3.19}$$

for $i = 1, 2, \ldots, s$, where $U_{ni}(\tau)$ can be obtained from the substitution of Eq. (3.18) into Eq. (3.19), and use of $u(0, \tau) = 0$, i.e., $u_0(\tau) = 0$ (cf. Eq. (2.3)). Such a substitution yields, after evaluating the expression so obtained at t_{ni}

$$U_{ni}(t_{ni}) = h_n \sum_{j=1}^{s} a_{ij} K(t_{ni}, Y_{nj}) + \sum_{m=0}^{n-1} h_m \sum_{j=1}^{s} b_j K(t_{ni}, Y_{mj}), \tag{3.20}$$

where we have assumed that the time step may be variable.

Substitution of Eq. (3.20) into Eq. (3.18) yields

$$\epsilon Y'_{ni} = g\left(Y_{ni}, h_n \sum_{j=1}^{s} a_{ij} K(t_{ni}, Y_{nj}) + \sum_{m=0}^{n-1} h_m \sum_{j=1}^{s} b_j K(t_{ni}, Y_{mj})\right), \tag{3.21}$$

and this approximation coincides with the one that results from applying the Pouzet-Volterra-Runge-Kutta method to Eq. (2.4) [7]. Furthermore, as shown by Hairer et al. [15, 16, 17], if f and K are sufficiently smooth and the step size is constant and the implicit Runge-Kutta method presented above is employed only in the outer layer, i.e., when the fast transients have died out, then the errors in the outer layer are $O(h^p) + O(\epsilon h^q)$ if $a_{si} = b_i$ for $i = 1, 2, \ldots, s$, or $O(h^{q+1})$, otherwise, where p and q are the classical order and the stage order $(1 \leq q < p)$, respectively, of the implicit

Runge-Kutta method. Moreover, for the outer solution, Hairer et al. [15] have shown that the errors are $O(h)$ for $p = q = 1$.

The implicit Runge-Kutta method described above was only employed to determine the solution of Eq. (2.1) or Eq. (2.4) in the outer layer, i.e., after the initial transients associated with the internal layer are over. In this paper, either the exact solution when available or the solution obtained with EPUM at $t = \sigma$ was used as initial condition for the implicit Runge-Kutta method. In the latter case, the resulting technique is a patching one and is hereafter referred to as EIRKO. Furthermore, we have used Radau IIA methods which satisfy $p = 2s - 1$ and $q = s$, and their global error is $O(h^{2s-1}) + O(\epsilon h^s)$ in the outer layer, for fixed step size. This behavior has been assessed by determining the solution in the outer layer with Radau IIA methods as a function of s and h and the results indicate that the global error is $O(h^{2s-1})$ for small p (or small s) or large step size, h, whereas it is $O(\epsilon h^s)$ for large p (or large s) or small h, as discussed below.

4. **RESULTS**

In this section, we present some sample results which have been obtained with the EIEO, EPUM and EIRKO formulations presented in this paper for some singularly-perturbed Volterra integro-differential equations, as well as comparisons with the results obtained with the exponentially-fitted methods developed by Salama and Bakr [35] and the author [29]. Salama and Bakr [35] also present comparisons with the results obtained with the backward Euler and trapezoidal methods for Eq. (2.1), as well as those corresponding to the outer solution of Eq. (2.1), i.e., to $\epsilon = 0$ in Eq. (2.1). This (leading-order) outer solution does not include the initial layer and the resulting equation can be solved numerically by means of, for example, the trapezoidal rule or Newton-Cotes quadrature.

In the two examples considered in this paper, we have determined the maximum-norm errors, i.e.,

$$E^N = \max_n |y_n^N - y(t_n)|, \qquad n = 1, 2, \ldots, N+1, \tag{4.1}$$

where $y(t_n)$ denotes the exact solution at $t = t_n$, and the convergence order p of the methods, i.e.,

$$p = \log_2 \left(\frac{E^N}{E^{2N}} \right). \tag{4.2}$$

Example 1. This example corresponds to

$$\epsilon y' + y - (1+\epsilon) \int_0^t y(s) ds = (1+\epsilon) e^{-1} - \epsilon, \qquad 0 < t \leq 1, \tag{4.3}$$

subject to $y(0) = 1 + e^{-1}$, which has the following exact solution

$$u(t) = \exp(t-1) + \exp\left(-\frac{t}{\epsilon}(1+\epsilon)\right), \tag{4.4}$$

and is a singularly-perturbed linear Volterra integro-differential equation [19] whose solution exhibits an initial layer at $t = 0$ of thickness $O(\epsilon)$. For this example, $a(t) = 1$ (cf. Eq. (2.1)) and, therefore, the problem of consistency between the outer analytical solution and that obtained from the exponential method presented in this paper does not arise (cf. Remark 1).

TABLE 1. Maximum norm errors E^N and convergence order p for the EIEO, BE, TR and EFS2 formulations as functions of $h = \frac{1}{N}$ and ϵ for Example 1, where BE, TR and EFS2 denote the backward Euler, trapezoidal and the exponential-fitted methods of Salama and Bakr [35] with $m = 2$.

Method	$N = \frac{1}{h}$	$\epsilon = 1$	$\epsilon = h$	$\epsilon = h^2$	$\epsilon = h^3$
		E (p)	E (p)	E (p)	E (p)
EIEO	32	1.11E-04 (2.00)	2.85E-03 (0.96)	3.68E-02 (0.96)	3.71E-02 (1.02)
EIEO	64	4.43E-05 (2.00)	1.46E-03 (0.98)	1.89E-02 (0.98)	1.83E-02 (1.03)
EIEO	128	1.11E-05 (2.04)	7.38E-04 (0.95)	9.59E-03 (0.99)	8.99E-03 (1.00)
EIEO	256	2.69E-06	3.81E-04	4.82E-03	4.50E-03
BE [35]	32	2.44E-02 (1.01)	1.35E-01 (0.02)	3.04E-02 (0.55)	1.69E-02 (1.02)
BE [35]	64	1.21E-02 (1.00)	1.33E-01 (0.01)	1.54E-02 (0.53)	7.92E-02 (1.01)
BE [35]	128	6.04E-03 (1.00)	1.33E-01 (0.00)	7.76E-03 (0.52)	3.93E-03 (1.00)
BE [35]	256	3.01E-03	1.32E-01	3.89E-03	1.96E-03
TR [35]	32	9.91E-05 (1.99)	3.69E-02 (0.04)	8.82E-01 (-0.09)	9.96E-01 (0.00)
TR [35]	64	2.47E-05 (2.00)	3.57E-02 (0.02)	9.39E-01 (-0.04)	9.99E-01 (0.00)
TR [35]	128	6.19E-06 (1.99)	3.51E-02 (0.01)	9.69E-01 (-0.02)	9.99E-01 (0.00)
TR [35]	256	1.54E-06	3.48E-02	9.84E-01	9.99E-01
EFS2 [35]	32	1.62E-06 (2.95)	2.46E-03 (0.99)	3.25E-02 (0.93)	3.51E-02 (0.99)
EFS2 [35]	64	2.10E-07 (2.97)	1.23E-03 (0.99)	1.69E-02 (0.97)	1.76E-02 (0.99)
EFS2 [35]	128	2.67E-08 (2.98)	6.20E-04 (0.99)	8.67E-03 (0.98)	8.83E-03 (0.99)
EFS2 [35]	256	3.36E-09	3.10E-04	4.38E-03	4.42E-03

Table 1 shows the maximum norm errors and the order of accuracy of EIEO as well as those of the backward Euler, trapezoidal and Salama and Bakr's [35] third-order accurate exponentially-fitted method which are denoted by BE, TR and EFS2, respectively. For fixed ϵ and $h > \epsilon$, the results shown in Table 1 (and others not presented here) indicate that BE and TR are first- and second-order accurate, respectively; however, for $\epsilon < h$, the accuracy and order of TR are lower than those of BE. The order of EIEO is two for $\epsilon = 1$, but decreases albeit it is near unity for $\epsilon < h$;

a similar comment applies to EFS2, although the accuracy of this method is higher than that of EIEO for $\epsilon = 1$. Table 1 also shows that the accuracy of EIEO is comparable but slightly lower than that of EFS2 for $\epsilon \leq h$. It must be pointed out that the accuracy of EFS2 is $O(h^3)$ when the inner layer is resolved, and this is consistent with the results shown in (the first column of) Table 1.

TABLE 2. Maximum norm errors E^N and convergence order p for the EPUM as functions of N and ϵ for Example 1.

	$\epsilon = 2^{-4}$	$\epsilon = 2^{-6}$	$\epsilon = 2^{-8}$	$\epsilon = 2^{-10}$
N	E (p)	E (p)	E (p)	E (p)
32	1.12E-03 (1.99)	1.34E-03 (2.02)	1.41E-03 (2.01)	1.43E-03 (2.02)
64	2.79E-04 (2.00)	3.33E-04 (2.00)	3.52E-04 (2.01)	3.55E-04 (2.01)
128	6.98E-05 (1.99)	8.32E-05 (1.99)	8.79E-05 (2.01)	8.86E-05 (1.99)
256	1.74E-05	2.09E-05	2.19E-05	2.22E-03

In Table 2, the maximum norm errors and order of EPUM are presented as functions of N and ϵ. This table clearly shown that EPUM is a second-order method which is almost uniformly convergent.

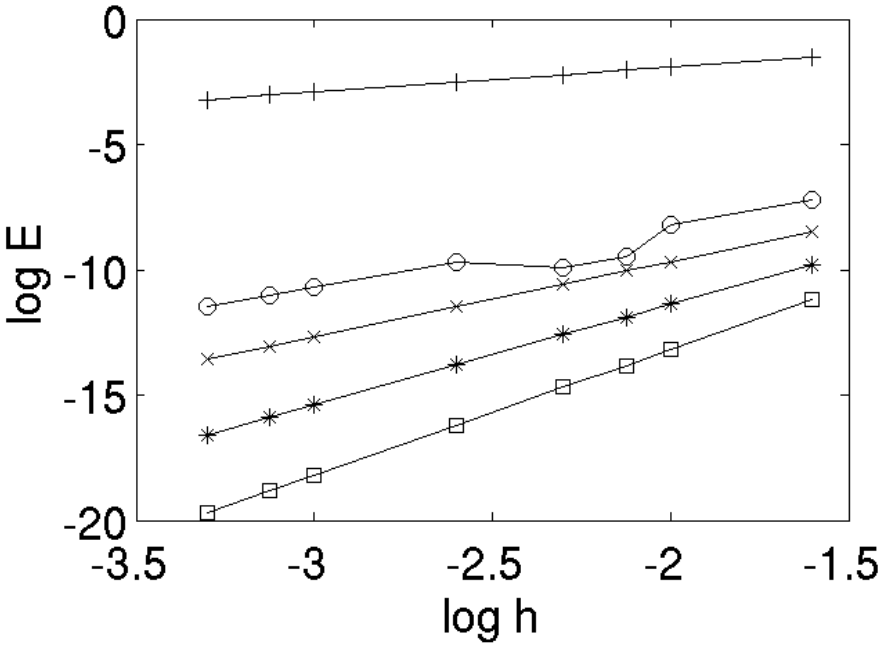

FIGURE 1. Maximum norm errors at $t = 0.5$ as functions of the constant step size, h, and stages of the implicit Runge-Kutta method for Example 1 with $\epsilon = 10^{-5}$. ($s = 1$: $+$; $s = 2$: $\circ$; $s = 3$: $\times$; $s = 4$: $*$; $s = 5$: $\square$.)

The maximum norm errors at $t = 0.5$ of the implicit Runge-Kutta-Radau II A method for Example 1 are shown in Figure 1 as functions of the (constant) step size in a log-log scale for $\epsilon = 10^{-5}$. The results reported in this figure as well as in Figure 2 were obtained by applying the Runge-Kutta method with the initial conditions at $t = \sigma$ as discussed above and, therefore, they do correspond to the outer layer.

The results exhibited in Figure 1 indicate that the errors of the implicit Runge-Kutta method decreases as the order is increased and increase as the step size is increased. For small s or large h, the error is $O(h^{2s-1})$, but, for large s or small h, the errors are $O(\epsilon h^s)$ in accordance with the errors estimates provided by Hairer et al. [15, 16, 17] for the outer layer of singularly-perturbed or stiff systems of ordinary differential equations. Note that the dependence of the maximum norm errors on ϵ discussed above is associated with the fact that, even though the implicit Runge-Kutta method has been used only in the outer layer, Eq. (2.4) depends on ϵ. This should be contrasted with the leading-order outer problem which is obtained by setting $\epsilon = 0$ in Eq. (2.1) and, therefore, the resulting equation does not depend on the small perturbation parameter.

Example 2. This example corresponds to

$$\epsilon y' + y + (1+\epsilon)\int_0^t y^2(s)ds = -\frac{1+\epsilon}{2\exp(2)} - \frac{\epsilon}{2}\left(1+\exp\left(-\frac{t}{\epsilon}(1+\epsilon)\right)\right)^2 + \frac{\epsilon-1}{2} + \frac{\epsilon+1}{2}\left(1+\exp(t-1)\right)^2 + \frac{2\epsilon(\epsilon+1)}{e}\left(1-\exp\left(-\frac{t}{\epsilon}\right)\right), \tag{4.5}$$

for $0 < t \leq 1$, subject to $y(0) = 1 + e^{-1}$, which has the following exact solution

$$y(t) = \exp(t-1) + \exp\left(-\frac{t}{\epsilon}(1+\epsilon)\right), \tag{4.6}$$

and is a singularly-perturbed nonlinear Volterra integro-differential equation [19] whose solution exhibits an initial layer at $t = 0$ of thickness $O(\epsilon)$. For this example, $a(t) = 1$ (cf. Eq. (2.1)) and, therefore, the problem of consistency between the outer analytical solution and that obtained from the exponential method presented in this paper does not arise (cf. Remark 1).

Table 3 shows similar trends to those found in Table 1, except that the errors of the EIEO and EFS2 formulations for Example 2 are larger than those for Example 1. Table 2 also shows that the errors of EIEO are larger than those of the exponentially-fitted method of Salama and Bakr [35] for $\epsilon = h$ because the latter has been fitted so that the resulting finite difference techniques are third-order accurate for fixed ϵ. However, the order of accuracy of this method becomes one for $\epsilon < h$ because, for such step sizes, this exponentially-fitted technique does not resolve the initial layer. Both the EFS2 and EIEO methods show an order of accuracy equal to one for $\epsilon < h$.

TABLE 3. Maximum norm errors E^N and convergence order p for the EIEO, BE, TR and EFS2 formulations as functions of $h = \frac{1}{N}$ and ϵ for Example 2, where BE, TR and EFS2 denote the backward Euler, trapezoidal and the exponential-fitted methods of Salama and Bakr [35] with $m = 2$.

Method	$N = \frac{1}{h}$	$\epsilon = 1$	$\epsilon = h$	$\epsilon = h^2$	$\epsilon = h^3$
		E (p)	E (p)	E (p)	E (p)
EIEO	32	2.45E-04 (2.03)	3.09E-03 (0.91)	4.01E-02 (0.95)	4.56E-02 (1.04)
EIEO	64	5.98E-05 (2.00)	1.65E-03 (0.97)	2.07E-02 (0.97)	2.22E-02 (1.02)
EIEO	128	1.50E-05 (2.00)	8.41E-04 (0.94)	1.06E-02 (0.97)	1.09E-02 (0.97)
EIEO	256	3.74E-06	4.39E-04	5.42E-03	5.55E-03
BE [35]	32	2.09E-02 (0.96)	1.42E-01 (0.05)	3.06E-02 (0.98)	8.32E-03 (0.99)
BE [35]	64	1.07E-02 (0.98)	1.37E-01 (0.02)	1.54E-02 (0.99)	4.17E-03 (0.99)
BE [35]	128	5.43E-03 (0.99)	1.34E-01 (0.01)	7.77E-03 (0.99)	2.09E-03 (0.99)
BE [35]	256	2.73E-03	1.33E-01	3.89E-03	1.04E-03
TR [35]	32	3.05E-04 (1.99)	3.89E-02 (0.08)	9.09E-01 (-0.06)	1.42E+00 (-0.09)
TR [35]	64	7.63E-05 (2.00)	3.67E-02 (0.04)	9.53E-01 (-0.03)	1.52E+00 (-0.05)
TR [35]	128	1.90E-06 (1.99)	3.56E-02 (0.02)	9.76E-01 (-0.01)	1.57E+00 (-0.02)
TR [35]	256	4.76E-06	3.50E-02	9.88E-01	1.60E+00
EFS2 [35]	32	1.30E-05 (2.98)	3.23E-03 (1.00)	2.09E-02 (0.94)	2.22E-02 (0.98)
EFS2 [35]	64	1.65E-06 (2.99)	1.62E-03 (1.00)	1.08E-02 (0.97)	1.12E-02 (1.00)
EFS2 [35]	128	2.07E-07 (2.99)	8.17E-04 (1.00)	5.54E-03 (0.98)	5.63E-03 (1.00)
EFS2 [35]	256	2.60E-08	4.10E-04	2.79E-03	2.82E-03

TABLE 4. Maximum norm errors E^N and convergence order p for the EPUM as functions of N and ϵ for Example 2.

	$\epsilon = 2^{-4}$	$\epsilon = 2^{-6}$	$\epsilon = 2^{-8}$	$\epsilon = 2^{-10}$
N	E (p)	E (p)	E (p)	E (p)
32	1.83E-03 (1.99)	1.89E-03 (2.02)	1.93E-03 (2.00)	1.94E-03 (2.02)
64	4.58E-04 (2.00)	4.71E-04 (1.99)	4.83E-04 (2.00)	4.82E-04 (1.99)
128	1.15E-04 (1.99)	1.18E-04 (1.99)	1.21E-04 (1.99)	1.21E-05 (1.99)
256	2.89E-05	2.96E-05	3.03E-05	3.04E-03

Table 4 indicates that EPUM is an almost second-order uniformly convergent method for Example 2 and the errors of this technique for Example 2 are larger than those for Example 1.

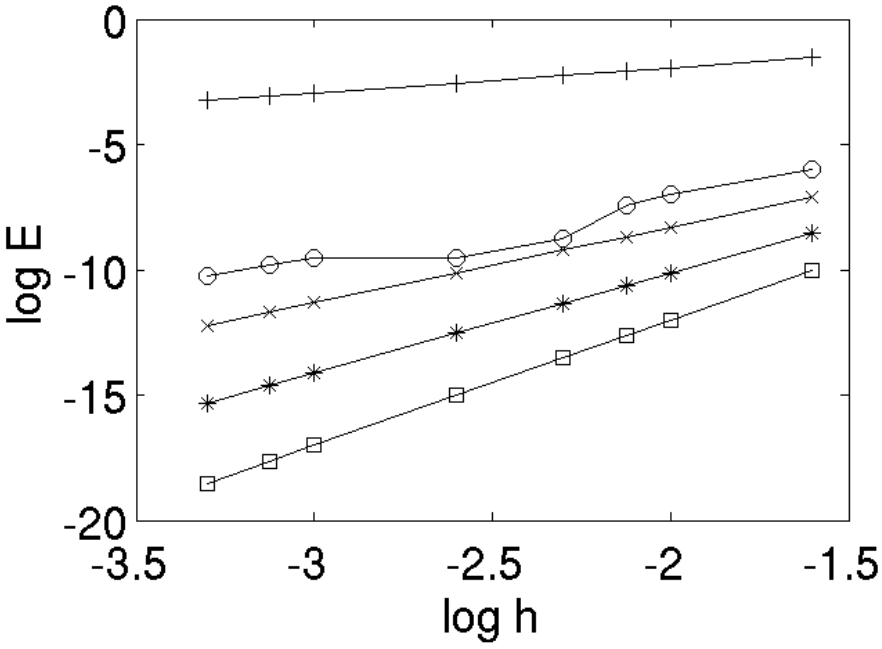

FIGURE 2. Maximum norm errors at $t = 0.5$ as functions of the constant step size, h, and stages of the implicit Runge-Kutta method for Example 2 with $\epsilon = 10^{-5}$. ($s = 1$: $+$; $s = 2$: $\circ$; $s = 3$: $\times$; $s = 4$: $*$; $s = 5$: $\square$.)

The maximum norm errors at $t = 0.5$ of the implicit Runge-Kutta-Radau II A method for Example 2 are shown in Figure 2 as functions of the (constant) step size in log-log scale for $\epsilon = 10^{-5}$, and exhibit similar trends to those of Figure 1, except that the errors for Example 2 are larger than those for Example 1.

5. CONCLUSIONS

An exponential method for singularly-perturbed Volterra integro-differential equations has been developed. The method is based on a piecewise linear approximation, results in a finite difference scheme of the exponential type, and is linearly stable. This technique has been implemented in a piecewise-uniform mesh and the resulting technique has been shown to provide a finite difference method which is independent of the small perturbation parameter in the inner layer and is almost second-order uniformly convergent.

Comparisons between the exponential method presented here and exponentially-fitted techniques which are third-order accurate for fixed values of the perturbation parameter indicate that the latter are slightly more accurate than the former for step sizes larger than the initial layer thickness, but the order of both techniques is equal to one when the initial layer is not resolved.

An implicit Runge-Kutta-Radau IIA method has also been developed to determine the solution in the outer layer starting with initial values provided by the exact solution, and it has been shown that the errors of this technique depend on both the step size and the order of the method when the number of stages is large or the step size is small, but they only depend on the step size when the number of stages is small or the step size is large, in accordance with theoretical estimates for singularly-perturbed systems of ordinary differential equations.

ACKNOWLEDGEMENTS

This research was partially financed by Project FIS2001-03191 from the Ministerio de Educación y Ciencia of Spain and fondos FEDER.

REFERENCES

[1] J. S. Angell and W. E. Olmstead, Singular perturbation analysis of an integrodifferential equation modelling filament stretching, *Z. Angew. Math. Phys. (ZAMP)*, 36:487–490, 1985.

[2] J. S. Angell and W. E. Olmstead, Singularly perturbed Volterra integral equations, *SIAM J. Appl. Math.*, 47:1–14, 1987.

[3] J. S. Angell and W. E. Olmstead, Singularly perturbed Volterra integral equations II, *SIAM J. Appl. Math.*, 47:1150–1162, 1987.

[4] A. Bijura, Singularly perturbed Volterra integral equations with weakly singular kernels. *Int. J. Math. Math. Sci.*, 30:129–143, 2002.

[5] A. Bijura, Singularly perturbed Volterra integro-differential equations, *Quest. Math.*, 25:229–248, 2002.

[6] A. Bijura, Rigorous results on the asymptotic solutions of singularly perturbed nonlinear Volterra integral equations, *J. Integ. Eqs. Applic.*, 14:119–150, 2002.

[7] H. Brunner and P. J. van der Houwen, *The Numerical Solution of Volterra Equations, CWI Monographs* Vol. 3, North-Holland, Amsterdam, The Netherlands, 1986.

[8] H. Brunner, *Collocation Methods for Volterra Integral and Related Functional Differential Equations*, Cambridge University Press, New York, 2004.

[9] J. Carroll, Sufficient conditions for uniformly second-order convergent schemes for stiff initial-value problems, *Comput. Math. Applics.*, 24:105–116, 1992.

[10] J. M. Cushing, *Integrodifferential Equations and Delay Models in Population Dynamics*, Springer-Verlag, New York, 1992.

[11] E. P. Doolan, J. J. H. Miller and W. H. A. Schilders, *Uniform Numerical Methods for Problems with Initial and Boundary Layers*, Boole Press, Dublin, Ireland, 1980.

[12] S. E. El-Gendi, Chebyshev solution of differential, integral and integro-differential equations, *Comput. J.*, 12:282–287, 1969.

[13] P. A. Farrell, Uniform and optimal schemes for stiff initial-value problems, *Comput. Maths. Appls.*, 13:925–936, 1987.

[14] P. A. Farrell, A. F. Hegarty, J. J. H. Miller, E. O'Riordan and G. I. Shishkin, *Robust Computational Techniques for Boundary Layers*, CRC Press, Inc., New York, 2000.

[15] E. Hairer, C. Lubich and M. Roche,Error of Runge-Kutta methods for stiff problems studied via differential algebraic equations, *BIT*, 28:678–700, 1988.

[16] E. Hairer and G. Wanner, *Solving Ordinary Differential Equations II: Stiff and Differential Algebraic Problems*, Springer-Verlag, Berlin, 1991.

[17] E. Hairer and G. Wanner, *Solving Ordinary Differential Equations II: Stiff and Differential Algebraic problems*, second revised edition, Springer-Verlag, Berlin, 1996.

[18] F. C. Hoppenstead, An algorithm for approximate solutions to weakly filtered synchronous control systems and nonlinerar renewal processes, *SIAM J. Appl. Math.*, 43:834–843, 1983.

[19] V. Horvat and M. Rogina, Tension spline collocation methods for singularly perturbed Volterra integro-differential and Volterra integral equations, *J. Comput. Appl. Math.*, 140:381–402, 2002.

[20] Q. Hu, Geometric meshes and their application to Volterra integral equations with singularities, *SIAM J. Numer. Anal.*, 18:151–164, 1998.

[21] A. M. Il'in, Differencing scheme for a differential equation with a small parameter affecting the highest derivative, *Math. Notes Acad. Sci. USSR*, 6:596–602, 1969.

[22] J.-P. Kauthen, Implicit Runge-Kutta methods for singularly perturbed integro-differential equations, *Appl. Numer. Math.*, 18:201–210, 1995.

[23] J. B. Keller and W. E. Olmstead, Temperature of a nonlinearly radiating semi-infinite solid, *Quart. Appl. Math.*, 29:559–566, 1972.

[24] W. Kelley and A. Peterson, *The Theory of Differential Equations: Classical and Qualitative*, Pearson Education, Inc., Upper Saddle River, New Jersey, 2004.

[25] A. S. Lodge, J. B. McLeod and J. A. Nohel, A nonlinear singularly perturbed Volterra integrodifferential equation occurring in polymer rheology, *Proc. Roy. Soc. Edinburgh, Sect. A.*, 80:99–115, 1978.

[26] W. E. Olmstead and R. A. Handelsman, Diffusion in a semi-infinite region with nonlinear surface dissipation, *SIAM Rev.*, 18:275–291, 1976.

[27] W. E. Olmstead and J. S. Angell, Singularly perturbed integral equations with end point boundary layers, *SIAM J. Appl. Math.*, 49:1567–1584, 1989.

[28] A. P. Orsi, Product integration for Volterra integral equations of the second kind with weakly singular kernels, *Math. Comp.*, 65:1201–1212, 1996.

[29] J. I. Ramos, Piecewise-quasilinearization techniques for singularly perturbed Volterra integro-differential equations, *Appl. Math. Comput.*, 188:1221–1233, 2007.

[30] J. I. Ramos, Linearized methods for ordinary differential equations, *Appl. Math. Comput.*, 104:109–129, 1999.

[31] J. I. Ramos, Linearization methods in classical and quantum mechanics, *Comp. Phys. Commun.*, 153:199–208, 2003.

[32] J. I. Ramos, Piecewise quasilinearization techniques for singular boundary-value problems, *Comp. Phys. Commun.*, 158:12–25, 2004.

[33] J. Reddingius, Notes on the mathematical theory of epidemics, *Acta Biotheor.*, 20:125–135, 1971.

[34] H.-G. Roos, M. Stynes and L. Tobiska, *Numerical Methods for Singularly Perturbed Differential Equations: Convection-Diffusion and Flow Problems*, Springer, Berlin, 2008.

[35] A. Salama and S. A. Bakr, Difference schemes of exponential type for singularly perturbed Volterra integro-differential problems, *App. Math. Modelling*, 31:866–879, 2007.

[36] M. Stynes and L. Tobiska, A finite difference analysis of a streamline diffusion method on a Shishkin mesh, *Numer. Algorithms*, 37:337–360, 1998.